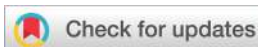


## PAPER



Cite this: *Food Funct.*, 2023, **14**, 5205

## Neuroprotective effect of aloe emodin against Huntington's disease-like symptoms in R6/1 transgenic mice†

Nan Yan,<sup>‡a</sup> Shuai Wang,<sup>‡b</sup> Haotian Gao,<sup>b</sup> Jiaqi Chen,<sup>b</sup> Jiahui Cao,<sup>c</sup> Pengsheng Wei,<sup>b</sup> Xue Li,<sup>b</sup> Ying Yu,<sup>d</sup> Yan Wang,<sup>e</sup> Yalin Niu,<sup>b</sup> Yijie Wang,<sup>b</sup> Shuyuan Liu<sup>\*‡c,f</sup> and Ge Jin<sup>‡c,f</sup>

Aloe emodin is a natural anthraquinone derived from aloe or rhubarb, showing anti-renal fibrosis, anti-atherosclerosis and anti-cancer effects. Aloe emodin also shows neuroprotective effects in ischemic stroke rats. Naturally, anthraquinone derivatives generally have the effect of inhibiting the transforming growth factor- $\beta$ 1 (TGF- $\beta$ 1) pathway. There is an increase in the calcium/calmodulin-dependent protein kinase II (CaMKII) and TGF- $\beta$ 1 levels in both Huntington's disease (HD) patients' brains and HD transgenic mice. Thus, we hypothesized that aloe emodin may inhibit the phosphorylation of CaMKII (p-CaMKII) and TGF- $\beta$ 1/sma- and mad-related protein (Smad) signaling in the brain, further preventing motor and cognitive dysfunction. Aloe emodin was orally administered to 10- to 20-week-old HD R6/1 transgenic mice. Aloe emodin improved the motor coordination of R6/1 transgenic mice in the rotarod test and attenuated visual recognition impairment in the novel object recognition test. Aloe emodin downregulated levels of the mutant huntingtin protein, p-CaMKII and TGF- $\beta$ 1, but not the TGF- $\beta$ 2 or TGF- $\beta$ 3 levels, in the brains of R6/1 mice. Aloe emodin could also inhibit neuronal apoptosis in the hippocampus of R6/1 mice. Altogether, these results indicated that aloe emodin prevents several HD-like symptoms through the inhibition of CaMKII/Smad and TGF- $\beta$ 1/Smad signaling in mice.

Received 11th January 2023,

Accepted 10th April 2023

DOI: 10.1039/d3fo00156c

rsc.li/food-function

## 1. Introduction

As a progressive neurodegenerative disease, Huntington's disease (HD) causes motor and cognitive dysfunction. The HD gene encodes huntingtin (Htt) and contains a cytosine-adenine-guanine (CAG) repeat in exon 1.<sup>1</sup> Abnormal expansion of this CAG repeat (>35) causes Htt to misfold. The mutant htt (mhtt) protein induces neuronal cell death, especially in the striatum and cerebral cortex. R6 transgenic mice are the most commonly used HD mouse model and express a truncated form of human Htt.<sup>2</sup>

As a multifunctional cytokine, TGF- $\beta$ 1 regulates neuronal cell survival and glial activation.<sup>3</sup> Parkinson's disease, Alzheimer's disease and HD patients display high TGF- $\beta$ 1 levels, especially in the blood vessels of the brain.<sup>3-5</sup> This high TGF- $\beta$ 1 level promotes inflammation, vascular hypertrophy, fibrosis, and the accumulation of extracellular matrix components.<sup>6</sup> Accordingly, TGF- $\beta$ 1 overexpression in mice causes neuroinflammation and cerebral vessel injury.<sup>7-9</sup>

CaMKII is an important protein kinase that promotes tau phosphorylation and memory formation. The dysfunction of CaMKII disturbs calcium signaling, induces neuronal cell death, and memory dysfunction. The literature also reports that Ca<sup>2+</sup>/CaMK levels are significantly enhanced in R6 HD transgenic mice and TgCRND8 AD transgenic mice.<sup>10,11</sup> This upregulation may promote reactive oxygen species generation and eventually contribute to exacerbation of the pathological phenotype. Therefore, we believe that the inhibition of CaMKII and TGF- $\beta$ 1 signaling may alleviate some of the pathogenesis pathogenetic routes of HD.

Aloe emodin (1,8-dihydroxy-3-hydroxymethyl anthraquinone) is a naturally occurring anthraquinone derived from aloe or rhubarb, that exhibits anti-renal fibrosis, anti-atherosclerosis and anti-cancer activities.<sup>12-14</sup> As a small molecule (MW = 270.24), aloe emodin can cross the blood-brain barrier.<sup>15</sup> Aloe

<sup>a</sup>School of Medical Applied Technology, Shenyang Medical College, Shenyang, 110034, P.R. China

<sup>b</sup>Basic Medical School, Shenyang Medical College, Shenyang, 110034, P.R. China

<sup>c</sup>School of Pharmacy, Shenyang Medical College, Shenyang, 110034, P.R. China.

E-mail: jinge1026@163.com, liushuyuan@symc.edu.cn

<sup>d</sup>Liaoning Medical Device Test Institute, Shenyang, 110171, P.R. China

<sup>e</sup>Department of Occupational and Environmental Health, School of Public Health, Shenyang Medical College, Shenyang, 110034, P.R. China

<sup>f</sup>Key Laboratory of Behavioral and Cognitive Neuroscience of Liaoning Province, Shenyang Medical College, Shenyang, 110034, P.R. China

† Electronic supplementary information (ESI) available. See DOI: <https://doi.org/10.1039/d3fo00156c>

‡ Co-first authors.

emodin also shows neuroprotective effects in ischemic stroke rats.<sup>15,16</sup> In this study, we first report the use of aloe emodin in R6/1 transgenic mice. Motor and cognitive functions were evaluated using several behavioral experiments. Body and brain weights were recorded after aloe emodin treatment. Then, we tested the expression of the mutant huntingtin protein, CaMKII and TGF- $\beta$ 1 signaling, after aloe emodin treatment.

## 2. Materials and methods

### 2.1. Animals

Male B6.Cg-Tg(HDexon1)61Gpb/JNju mice were purchased from Nanjing Biomedical Research Institution of Nanjing University (China), and wild-type mice were used as controls. B6/JGpt-Tg(hHTT-CAG130)90/Gpt mice at 7 weeks old were purchased from GemPharmatech (China), and wild-type mice were used as controls. Mice were housed under a 12 h light/dark cycle and had free access to food and water. All animal studies were performed in strict accordance with the P.R. China legislation on the use and care of laboratory animals and the guidelines established by the Institute for Experimental Animals at Shenyang Medical College.

### 2.2. Drug and treatment schedule

**Experiment A.** The mice were divided into a control group (WT,  $n = 8$ ), an R6/1 mouse group (model,  $n = 10$ ) and an R6/1 mouse and aloe emodin 150 mg kg<sup>-1</sup> dose group (aloe emodin,  $n = 9$ ). Aloe emodin (purity  $\geq 98\%$ ) was purchased from MedChemExpress (USA) and dissolved in 0.5% CMC-Na. Ten-week-old mice were given aloe emodin by gavage administration, once a day until the mice were sacrificed. After the test, the right half of the brain was used for immunohistochemical staining. The left striatum was used for PCR and EM48 expression analysis. The left cerebral cortex was used to test the TGF- $\beta$ , CaMKII and Smad2/3 expression; the left hippocampus was used to test the Bcl-2 and Bax expression. One hundred mg kg<sup>-1</sup> aloe emodin could prevent nerve injury and neuroinflammation in ischemic stroke rats.<sup>15</sup> We converted the equivalent dose according to the body surface area of rats and mice and determined that the dose for mice was about 150 mg kg<sup>-1</sup>.

**Experiment B.** The mice were divided into a control group (WT, 4 male and 4 female), a B6-hHTT130-N mouse group (model, 3 male and 4 female), a B6-hHTT130-N mouse and aloe emodin 150 mg kg<sup>-1</sup> dose group (aloe emodin, 3 male and 4 female) and a B6-hHTT130-N mouse and fisetin 20 mg kg<sup>-1</sup> dose group (fisetin, 4 male and 3 female). Fisetin (purity  $\geq 98\%$ ) was purchased from MedChemExpress (USA) and dissolved in 0.5% CMC-Na. Eight-week-old mice were given aloe emodin or fisetin by gavage administration, once a day, until 12 weeks old to test the rotarod performance and the expression of mHtt in the striatum. The dose of fisetin was based on the studies of Ahmad *et al.* and Khatoun *et al.*<sup>17–19</sup>

### 2.3. Hindlimb clasping test

R6/1 mice exhibit progressive hindlimb clasping behavior, which is a marker of motor impairment observed in many neurodegenerative disease animal models. Clasping behavior was tested at 20 weeks old, as described by Guyenet *et al.*<sup>20</sup> The mouse was suspended by the tail, approximately 40 cm above its cage, and the hindlimbs were observed for 10 s. A score of “0” was defined when two hindlimbs were splayed from the abdomen. A score of “1” was defined when one hindlimb was retracted toward the abdomen for more than 5 s. A score of “2” was defined when two hindlimbs were partially retracted toward the abdomen for more than 5 s. A score of “3” was defined when two hindlimbs were entirely retracted toward the abdomen for more than 5 s. These neurological scores were used for comparative analyses.

### 2.4. Grip strength test

The mice were tested at 4-week intervals from 8 weeks of age to 20 weeks of age. The back of each mouse was scruffed back and their front paws were allowed to grab the grip bars, which were connected to a force sensor (Shanghai XinRuan Information Technology Co., Ltd). The mice were pulled back until they lost their grip. This process was performed three times, and the average value was used for comparative analyses.<sup>21</sup>

### 2.5. Rotarod test

The mice were tested at 2-week intervals from 8 weeks of age to 20 weeks of age. Before the test, the mice were habituated to the equipment (Shanghai XinRuan Information Technology Co., Ltd). On the test day, the test was performed three times at 30 rpm for 180 s, and the average latency to fall values were used for comparative analyses.<sup>21</sup> The mice were allowed to rest for at least 1 h between three tests.

### 2.6. Novel object recognition test

The preferential index (PI) was used to evaluate memory recall and visual recognition function in the novel object recognition test, which was performed when the mice were 20 weeks old.<sup>21</sup> PI was calculated as [time spent exploring novel object/total exploration time].

### 2.7. Reverse transcriptase-polymerase chain reaction (RT-PCR)

Total RNA from the striatum was extracted using TRIzol. RNA (2.0  $\mu$ g) was reverse-transcribed using a cDNA synthesis system. cDNA products were amplified by PCR with specific primers for mHtt (F: GGCTGAGGAAGCTGAGGAG; R: CCGCTCAGGTTCTGCTTTTA) and  $\beta$ -actin (F: CTGTGCCCATCT-ACGAGGGCTAT; R: TTTGATGTCACGCACGATTTC). Amplification was performed in a thermal cycler (BIOER, Life Express, China) under the following conditions: initial heating at 95 °C for 5 min followed by 40 cycles of denaturation at 95 °C for 15 s, annealing at 50 °C for 20 s, extension at 72 °C for 30 s, and then final extension at 25 °C for 5 min. The amplified PCR products were separated on

1.5% agarose gels and then visualized using ethidium bromide under UV light. The band intensity was quantified using Gel-Pro-Analyzer software.

### 2.8. Quantitative real-time PCR (qPCR)

Total RNA from the striatum was extracted using TRIzol. RNA (2.0 µg) was reverse-transcribed using a cDNA synthesis system according to the manufacturer's protocol (Beyotime Biotechnology, China). The cDNA was amplified using an SYBR Green PCR kit (Solarbio, China) on an Exicycler 96 real-time PCR detection system (BIONEER, Korea). The  $2^{-\Delta\Delta C_t}$  was used for fluorescence quantitative PCR analysis. All the experiments were performed under equal conditions and repeated three times. The sequence-specific primers were synthesized as follows: mHtt (F: ATGGCGACCCTGGAAAAGCT; R: TGCTGCTGGAAGGACTTGAG) and  $\beta$ -actin (F: CTGTGCCCATCTACGAGGGCTAT; R: TTTGATGTC-ACGCACGATTTC).

### 2.9. Immunohistochemistry

The mouse brains were routinely processed for paraffin embedding and cut into 5 µm-thick sections. The sections were incubated with huntingtin protein (1:100, Millipore mab5374, clone mEM48, reacts with the mutant huntingtin protein in HD patients and in transgenic animals that express different numbers of repeats from 82 to 150 glutamines; thus, it should recognize different forms of the mutant huntingtin protein) or the NeuN (1:500, Abcam ab177487, USA) antibody at 4 °C overnight. The sections were washed in PBS, incubated with the biotin-labeled secondary antibody (1:100, Boster BA1001, China) at 37 °C for 30 min, treated with the avidin-biotin enzyme reagent, and visualized using a DAB kit. The intensity and positive area of each section were quantified using ImageJ software.

### 2.10. Immunofluorescence

Five µm-thick sections were incubated with the MBP (1:100, Proteintech 10458-1-AP, China) antibody at 4 °C overnight. The sections were washed in PBS, incubated with the biotin-labeled secondary antibody (1:100, Boster BA1001, China) at 37 °C for 30 min, treated with the secondary antibody TRITC-conjugated goat anti-rabbit IgG (H + L) (1:300, ProteinTech, China). Then, the brain slices were sealed with an anti-fluorescence quenching blocking agent containing DAPI and observed with a fluorescence microscope (Nikon, Japan). The positive area of each section was quantified using ImageJ software.

### 2.11. HE staining

Five µm-thick sections were stained with hematoxylin staining solution and alcohol eosin solution. After staining, the sections were dehydrated in anhydrous ethanol and treated with xylene. Then, the sections were dipped in resinous medium, mounted on a cover glass, and observed with an optical microscope.

### 2.12. TUNEL staining

TUNEL staining was undertaken using an In Situ Cell Death Detection Kit (Roche Diagnostics). Five µm-thick paraffin sections were incubated for 30 min at 37 °C with POD. After washing with PBS, diaminobenzidine was used to visualize the signals. The TUNEL positive cells were observed using an optical microscope.

### 2.13. TGF- $\beta$ content assay

The TGF- $\beta$ 1,  $\beta$ 2 and  $\beta$ 3 contents were tested using a U-PLEX TGF- $\beta$  Combo mouse assay kit (MSD K15242K, USA) according to the manufacturer's protocol. This assay kit contains 3 biomarkers grouped together for ordering convenience. The absorbance was measured at a wavelength of 620 nm using a microplate reader (MSD QuickPlex SQ120, USA).

### 2.14. Western blotting

Brain protein samples (40 µg) were electrophoresed on SDS-PAGE gels and then transferred to PVDF membranes. The membranes were blocked in 5% skim milk for 2 h at room temperature and incubated with primary antibodies against huntingtin (EM48, 1:100, Millipore, USA), p-CaMKII (T286), CaMKII, p-DARPP32 (T34), dopamine D1 and D2 receptors (1:1000, Abcam, USA), p-smad2 (s465 + s467)/p-smad3 (s423 + s425), Smad2/3 (1:500, Wanleibio, China), Bcl-2 (1:500, Wanleibio, China), Bax (1:500, Wanleibio, China) and  $\beta$ -actin (1:1000, Santa Cruz, USA) at 4 °C overnight and then incubated with secondary antibodies for 2 h at room temperature. Protein bands were visualized using an ECL kit. The band intensity was quantified using densitometry with ImageJ software.

### 2.15. Molecular docking

The crystal structure of the CaMKII holoenzyme (PDB ID: 3SOA) in the complex with aloe emodin (PubChem Compound, <https://pubchem.ncbi.nlm.nih.gov/>) was used for molecular modeling. AutodockVina 1.2.2 was used to perform docking calculations. For docking analysis, the protein and molecular files were converted into PDBQT format with all water molecules excluded and polar hydrogen atoms added. The grid box was centered to cover the domain of each protein and to accommodate free molecular movement. The grid box was set to 30 Å × 30 Å × 30 Å, and the grid point distance was 0.05 nm. Molecular docking studies were performed by Autodock Vina 1.2.2 (<https://autodock.scripps.edu/>).

### 2.16. Statistical analysis

The data were analyzed using SPSS 21.0. The statistical significance was determined using one-way ANOVA followed by Fisher's LSD multiple comparisons test with homogeneity of variance or Dunnett's T3 test with heterogeneity of variance. Experimental data are represented as means  $\pm$  SD.  $p < 0.05$  indicates statistical significance.

### 3. Results

#### 3.1. Effects of aloe emodin on body weight, neurological scores, motor and cognitive dysfunction in R6/1 mice

The body weight of R6/1 mice, which was used as an index of general health, progressively decreased at age 15 to 20 weeks, from  $21.90 \pm 2.72$  g to  $18.7 \pm 2.39$  g ( $p < 0.01$ , Fig. 1a). Aloe emodin

could not prevent against the body weight loss of R6/1 mice. Compared to the control group, the neurological scores were significantly decreased in R6/1 mice, and  $150 \text{ mg kg}^{-1}$  aloe emodin prevented hindlimb clasp symptoms, but the difference was not significant ( $p = 0.126$ , Fig. 1b and c). R6/1 mice exhibited a decrease in fall latency times from 14 to 20 weeks in the rotarod test, which indicated that R6/1 mice showed motor coordination

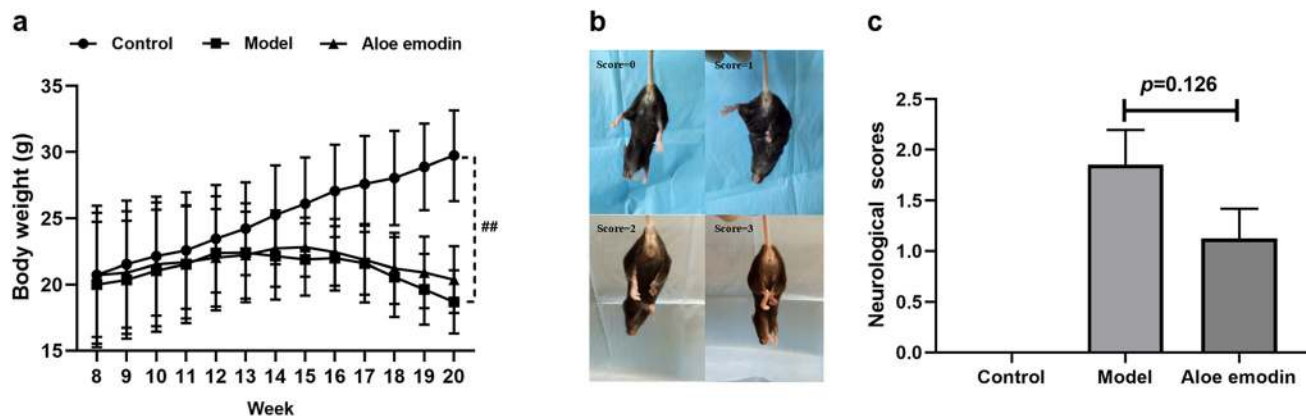


**Fig. 1** Effect of aloe emodin on the body weight and neurological scores in R6/1 mice. R6/1 mice exhibited a progressive decrease in body weight from 8 to 20 weeks of age (a) and obvious hindlimb clasp symptoms at 20 weeks old (b and c). Aloe emodin could not prevent the body weight loss (a). Aloe emodin decreased neurological scores, but the difference was not significant (b and c). All results are expressed as the mean  $\pm$  SD or SEM (neurological scores).  $n = 7-10$ ;  $##p < 0.01$  vs. control.

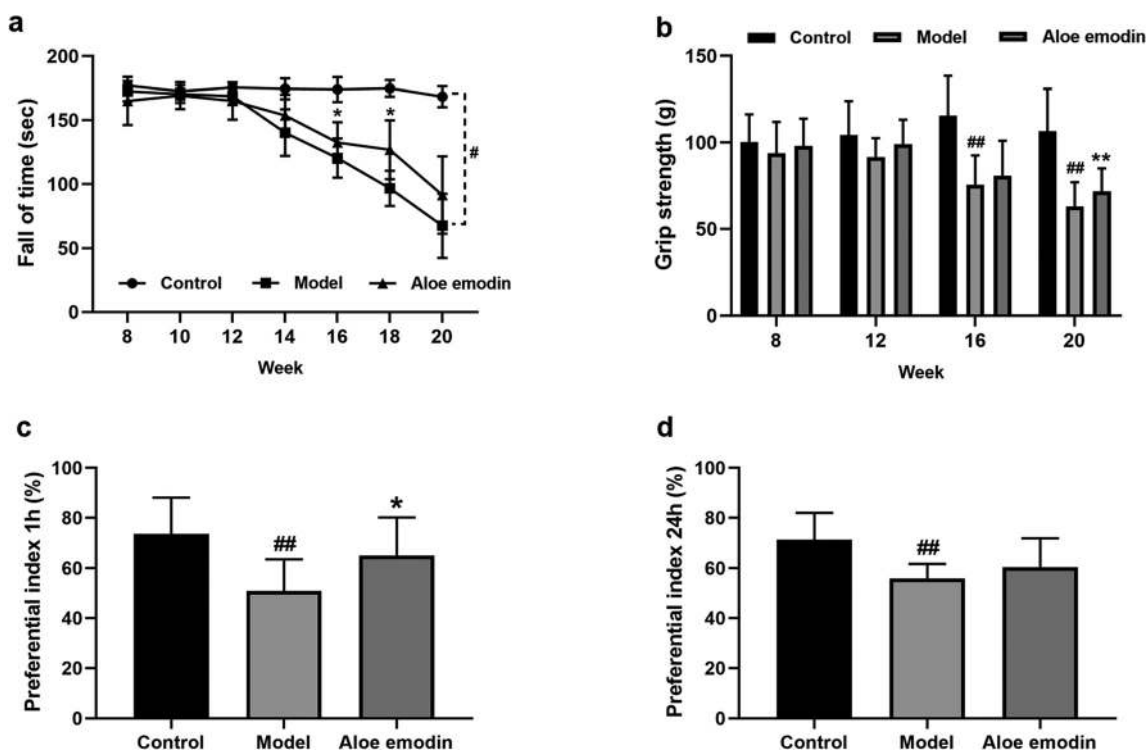


**Fig. 2** Effect of aloe emodin on motor and cognitive dysfunction in R6/1 mice. R6/1 mice exhibited a progressive decrease in the fall latency time in the rotarod test (a), muscle strength weakness in the grip strength test (b), memory recall and visual recognition deficits in the novel object recognition test (c and d) compared to the control mice. Aloe emodin improved the performance of the R6/1 mice in the rotarod test, grip strength test and cognitive deficits in the novel object recognition test from 16 weeks of age. All results are expressed as the mean  $\pm$  SD.  $n = 7-10$ ;  $#p < 0.05$ ,  $##p < 0.01$  vs. control;  $*p < 0.05$ ,  $**p < 0.01$  vs. model.

deficits ( $p < 0.05$ , Fig. 2a). Compared to the model group, aloe emodin significantly attenuated this decrease at 16 and 18 weeks ( $p < 0.05$ , Fig. 2a). The grip strength was gradually decreased in 16- to 20-week-old R6/1 mice, from  $100.14 \pm 12.79$  g to  $60.16 \pm 15.23$  g ( $p < 0.01$ , Fig. 2b). Compared to the model group, aloe emodin attenuated muscle strength weakness at 20 weeks of age ( $p < 0.01$ , Fig. 2b). Thus, aloe emodin attenuated motor dysfunction in the rotarod test of R6/1 mice. Furthermore, we used another HD transgenic mouse model, B6-hHTT130-N mice, to reconfirm the effect of aloe emodin on motor dysfunction. Compared to the model group, aloe emodin significantly increased the fall latency times of 12-week-old B6-hHTT130-N mice in the rotarod test ( $p < 0.01$ , ESI Fig. 1†). The polyphenol fisetin decreases the expression of mHtt, improves the rotarod performance and increases the lifespan in the R6/2 HD transgenic mice.<sup>22</sup> Therefore, we used fisetin as a positive control in this study. We found that fisetin could also prevent motor coordination deficits of 12-week-old B6-hHTT130-N mice in the rotarod test ( $p < 0.05$ , ESI Fig. 1†).

Cognitive dysfunction, especially recall memory dysfunction, appears even before motor dysfunction in HD patients and mouse models. Therefore, the novel object recognition test was used to evaluate memory recall and visual recognition impairments in R6/1 mice. Compared to the control group, the PI value at 1 h was decreased in 20-week-old R6/1 mice ( $p < 0.01$ , Fig. 2c). Similar results were observed in the PI value at 24 h ( $p < 0.01$ , Fig. 2d). Aloe emodin prevented the decrease in PI at 1 h ( $p < 0.05$ , Fig. 2c).

### 3.2. Effect of aloe emodin on brain injury in R6/1 mice

After the behavioral test, the mouse brains were weighed to evaluate the neuroprotective effect of aloe emodin. R6/1 mice exhibited lighter brain weights than the control group mice

( $p < 0.01$ , Fig. 3a). Aloe emodin slightly attenuated this decrease in brain weight, but the effect was not significant ( $p = 0.190$ , Fig. 3a). HE staining was used to determine the survival of striatal cells. The outline of cells was unclear and arranged irregularly in R6/1 mice. Aloe emodin prevented pathological damage (Fig. 3b). Immunohistochemistry of the neuronal marker neuronal nuclear antigen (NeuN) was used to evaluate the neuronal injury in the striatum. Compared to the control group, the numbers of NeuN positive cells were significantly decreased in the model group. Aloe emodin could significantly increase the NeuN covered area ( $p < 0.05$ , Fig. 3c and d).

Dopamine- and cAMP-regulated phosphoprotein 32 kDa (DARPP32) is a mediator of dopaminergic signaling in cells. Dopamine receptor activates PKA, and further promotes the phosphorylation of DARPP32. The literature reported that levels of phosphorylation of DARPP32 were significantly decreased in HD patients and mouse models.<sup>23,24</sup> In this study, compared with the model group, aloe emodin significantly increased the expression of D1R, D2R and p-DARPP32 levels in the striatum ( $p < 0.05$ , Fig. 4a–d).

### 3.3. Effect of aloe emodin on the expression of mHtt, TGF- $\beta$ and CaMKII signaling in R6/1 mice

Mutant htt induces neuronal cell death, particularly in the striatum and cerebral cortex. Therefore, we tested the effect of aloe emodin on mHtt. In experiment A, aloe emodin decreased the expression of mHtt to 40% in the striatum (WB,  $p < 0.01$ ; IHC mean IntDen,  $p < 0.01$ ; IHC covered area,  $p < 0.05$ , Fig. 5a and d–f). To investigate whether aloe emodin regulates mHtt at the transcriptional level, we used RT-PCR and qPCR to test the mRNA levels in R6/1 mouse brain samples. We found that

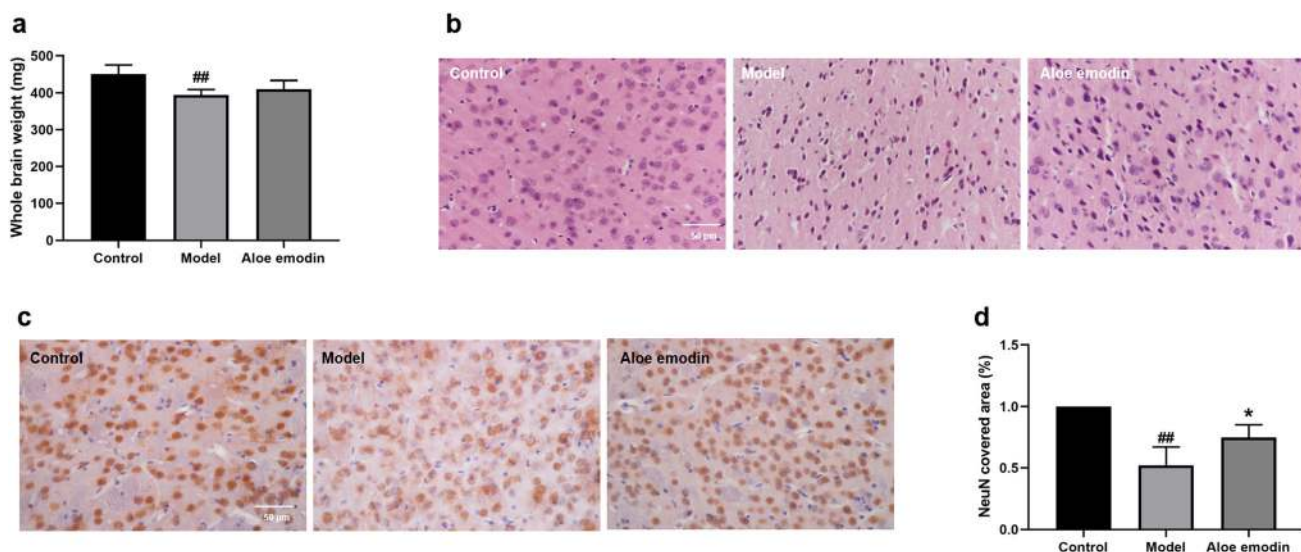


**Fig. 3** Effect of aloe emodin on brain injury in R6/1 mice. R6/1 mice exhibited a decrease in brain weight (a) compared to control mice. Aloe emodin slightly prevented the decrease in brain weight, but the difference was not significant. Aloe emodin improved cell morphology in the striatum, as shown by HE staining (b). Aloe emodin also significantly increased the expression of neuronal marker NeuN in the striatum (c and d). All results are expressed as the mean  $\pm$  SD. Brain weight,  $n = 7-8$ ; HE and IHC,  $n = 4$ . ## $p < 0.01$  vs. control; \* $p < 0.05$  vs. model.

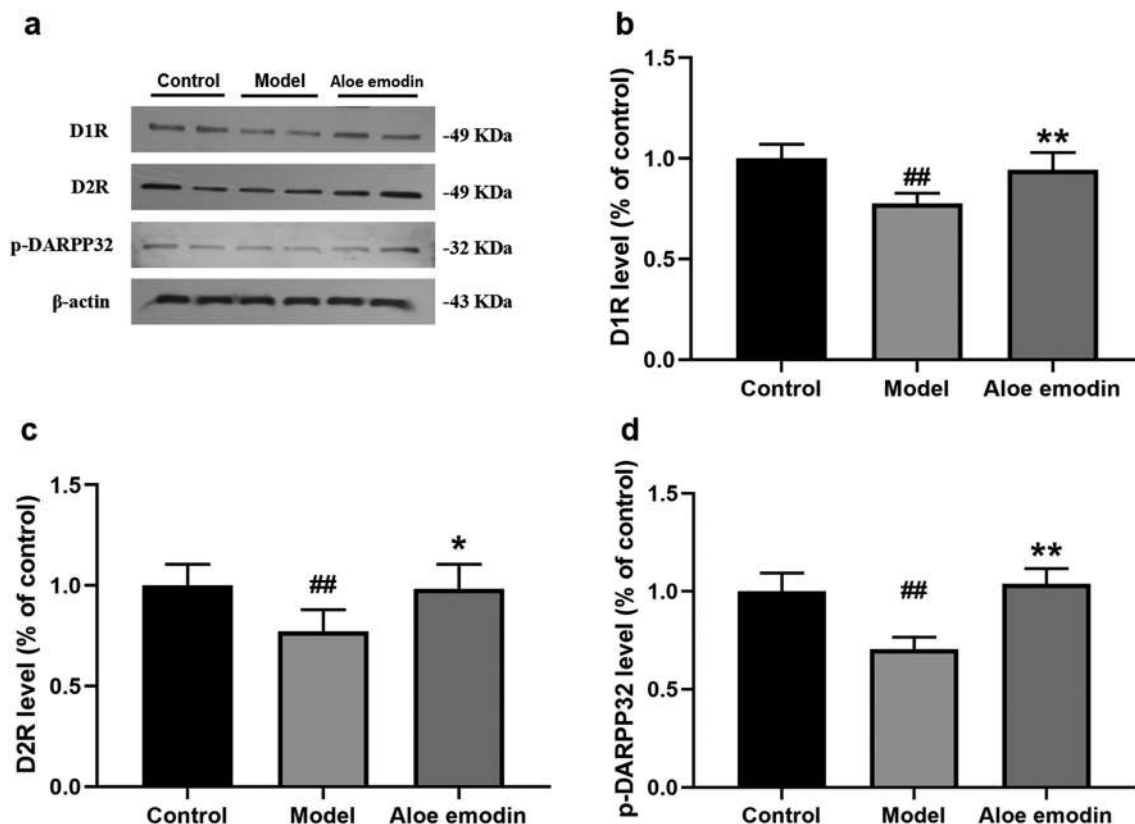


**Fig. 4** Effect of aloe emodin on dopamine receptor and DARPP32. Aloe emodin treatment for 10 weeks significantly ameliorated the reduced expression of D1R, D2R and the p-DARPP32 (T34) level in the striatum of the R6/1 mice (a). Quantification of the band densities of D1R, D2R and p-DARPP32 after aloe emodin treatment (b,c and d). Maybe aloe emodin can protect dopaminergic neurons against mHtt-induced excitotoxicity. All results are expressed as the mean  $\pm$  SD.  $n = 5$ . ## $p < 0.01$  vs. control; \* $p < 0.05$ , \*\* $p < 0.01$  vs. model.

aloe emodin did not change the mRNA level of mHtt ( $p > 0.05$ , Fig. 5b and c). Perhaps aloe emodin only inhibits mHtt at the protein level. In experiment B, we obtained similar experimental results to those of experiment A, where aloe emodin and fisetin significantly decreased the protein expression of mHtt in the striatum of the B6-hHTT130-N mice (mean IntDen,  $p < 0.01$ , ESI Fig. 2†).

Compared to the model group, TGF- $\beta$ 1 and p-CaMKII levels in the aloe emodin group were significantly decreased to  $8.19 \pm 1.08 \text{ pg mg}^{-1}$  and 70% ( $p < 0.05$ , Fig. 6a, d and e); aloe emodin also decreased the p-Smad 2/3 level to 78% ( $p < 0.01$ , Fig. 6d and f) in the cerebral cortex. Aloe emodin treatment could not prevent the decrease in the contents of TGF- $\beta$ 2 ( $p > 0.05$ , Fig. 6b), while no significant differences in the contents of TGF- $\beta$ 3 were observed among the groups ( $p > 0.05$ , Fig. 6c). Thus, aloe emodin inhibited mHtt expression and TGF- $\beta$ 1 and CaMKII signaling and prevented neuronal cell death in R6/1 mice. Both striatum and cerebral cortex are the main injury sites of HD but mice striatum is a very small tissue, which is not enough to detect all experimental indicators. Therefore, we tested TGF- $\beta$ 1 and p-CaMKII levels in the cerebral cortex, not in the striatum.

To evaluate the affinity of aloe emodin for its target, we performed molecular docking analysis. The binding poses and interactions of aloe emodin with CaMKII were obtained with

Autodock Vina v.1.2.2 and binding energy was generated. The result showed that aloe emodin had low binding energy of  $-7.18 \text{ kcal mol}^{-1}$ , indicating highly stable binding. The target protein was bound to aloe emodin through visible hydrogen bonding and strong electrostatic interactions; moreover, hydrophobic pocket of target proteins were occupied successfully by aloe emodin (Fig. 7).

#### 3.4. Effect of aloe emodin on apoptosis in the hippocampal area of R6/1 mice

We found that aloe emodin attenuated memory recall and visual recognition impairments of R6/1 mice in the novel object recognition test. Compared with the striatum, the hippocampus is more closely related to learning and memory. Thus, maybe aloe emodin could prevent or delay hippocampal-dependent cognitive deficits. Therefore, we tested the effect of aloe emodin on apoptosis in the hippocampus of R6/1 mice. First, we observed the expression of the myelin basic protein (MBP) in the hippocampal CA1 region, because it regulates neuronal membrane integrity and axonal regeneration.<sup>25,26</sup> Compared to the control group, the expression of MBP was significantly decreased in the model group ( $p < 0.05$ , Fig. 7a and b). Aloe emodin could prevent this decrease of MBP, which was comparable with the model group

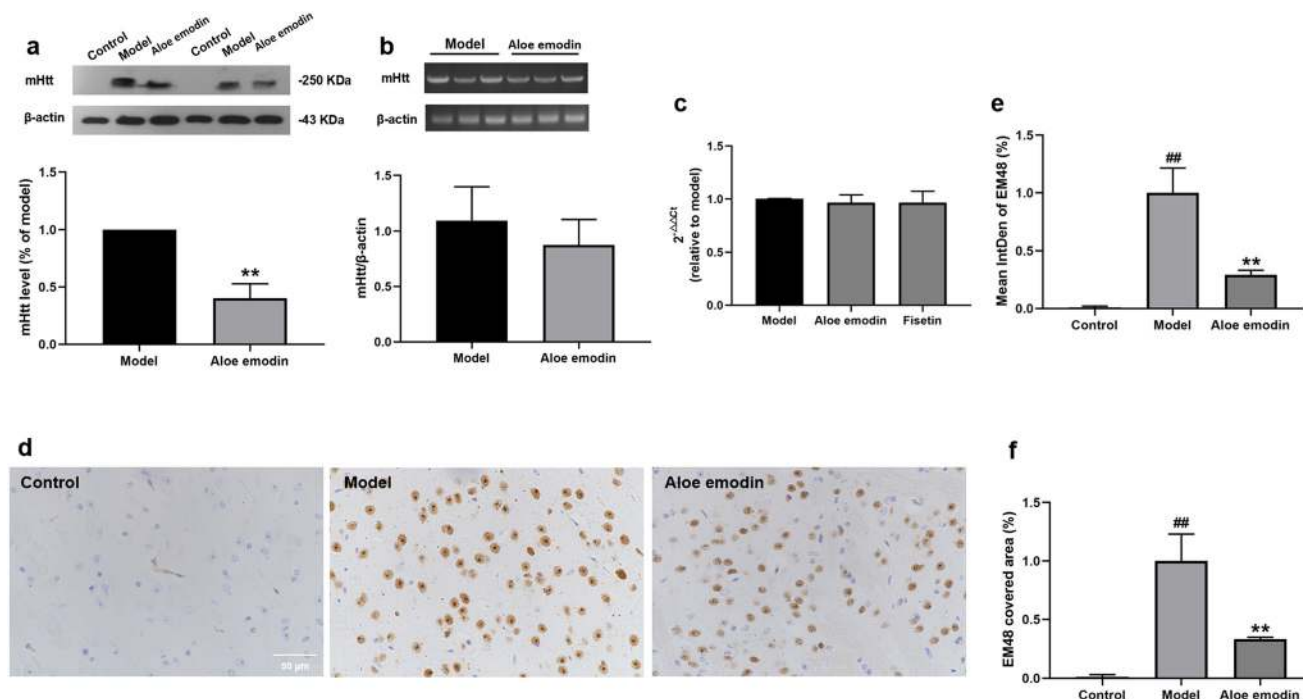


**Fig. 5** Effect of aloe emodin on the protein and mRNA levels of mHtt in the striatum of R6/1 mice. Aloe emodin treatment for 10 weeks significantly decreased the expression of mHtt (a) by WB, and the intensity and positive area of EM48-positive cells (d–f) in the striatum by IHC. However, aloe emodin did not change the mRNA levels of mHtt in the striatum (b and c). Perhaps aloe emodin only inhibits mHtt at the protein level. All results are expressed as the mean  $\pm$  SD. WB,  $n = 5$ ; IHC,  $n = 4$ , bar = 30  $\mu\text{m}$ ; PCR,  $n = 3$ . ## $p < 0.01$  vs. control; \*\* $p < 0.01$  vs. model.

( $p < 0.05$ , Fig. 7a and b). Neuronal degeneration and loss are the contributors to cognitive dysfunction. To evaluate whether aloe emodin can prevent mHtt-induced neuronal apoptosis, we used TUNEL staining to test the anti-apoptosis effect of aloe emodin. Compared to the control group, the number of apoptotic cells was significantly increased in the hippocampal CA1 region of the model group mice, which means that mHtt induced DNA breaks in the hippocampal neuron ( $p < 0.01$ , Fig. 7c and d). Also, with aloe emodin treatment, the number of apoptotic cells obviously decreased ( $p < 0.05$ , Fig. 7c and d). The endogenous apoptosis pathway starts from the pro-apoptotic protein Bax. After receiving the apoptosis signal, Bax transfers to mitochondria and promotes the release of cytochrome c. The anti-apoptotic protein Bcl-2 can prevent the effect of Bax. Aloe emodin significantly increased the expression of Bcl-2 and decreased the expression of Bax in the hippocampus (Bcl-2,  $p < 0.01$ ; Bax,  $p < 0.05$ , Fig. 7e–g). These results indicated that aloe emodin prevented neuronal apoptosis in the hippocampus of R6/1 mice.

## 4. Discussion

Aloe emodin is a natural anthraquinone derivative and an active ingredient of herbs.<sup>27</sup> Aloe emodin decreases the infarct size and behavioral score, and prevents neuroinflammation of middle cerebral occlusion reperfusion rats.<sup>15,16</sup> Aloe emodin also protects oxygen and glucose deprivation reperfusion-

induced SH-SY5Y cell death and decreases the inflammatory cytokine levels in LPS-treated BV2 cells.<sup>15</sup> But, the effect of aloe emodin on neurodegenerative diseases has not been fully reported. The literature has reported that R6/1 mice show motor and cognitive dysfunction beginning at around 14 weeks, and this dysfunction lasts more than 20 weeks.<sup>28,29</sup> Therefore, in the present study, we used the rotarod test and grip strength test to assess motor deficits and muscle strength in 8–20-week-old R6/1 mice. We found progressive deterioration of locomotor coordination and muscular weakness in the forelimb of R6/1 mice, which was prevented by aloe emodin. Similar results were found in supplementary experiments; aloe emodin could attenuate motor coordination deficits of 12-week-old B6-hHTT130-N mice in the rotarod test. Cognitive dysfunction, especially neuron and synapse loss-induced serious recall memory dysfunction, occurs even before motor dysfunction in HD patients and mouse models.<sup>28,30,31</sup> In this study, aloe emodin increased the preferential index in novel object recognition at 1 h, indicating that aloe emodin improves recall memory. Although not significant, aloe emodin tended to attenuate the performance in the novel object recognition test at 24 h.

Mutant huntingtin decreases glutamate uptake in the brains, and increases neuronal susceptibility to excitotoxicity.<sup>31</sup> We found that aloe emodin reduced mHtt at the protein level, but not mRNA in the striatum. Aloe emodin also ameliorated the reduced expression of D1R, D2R and p-DARPP32. Obvious dopaminergic alterations were found in HD patients.

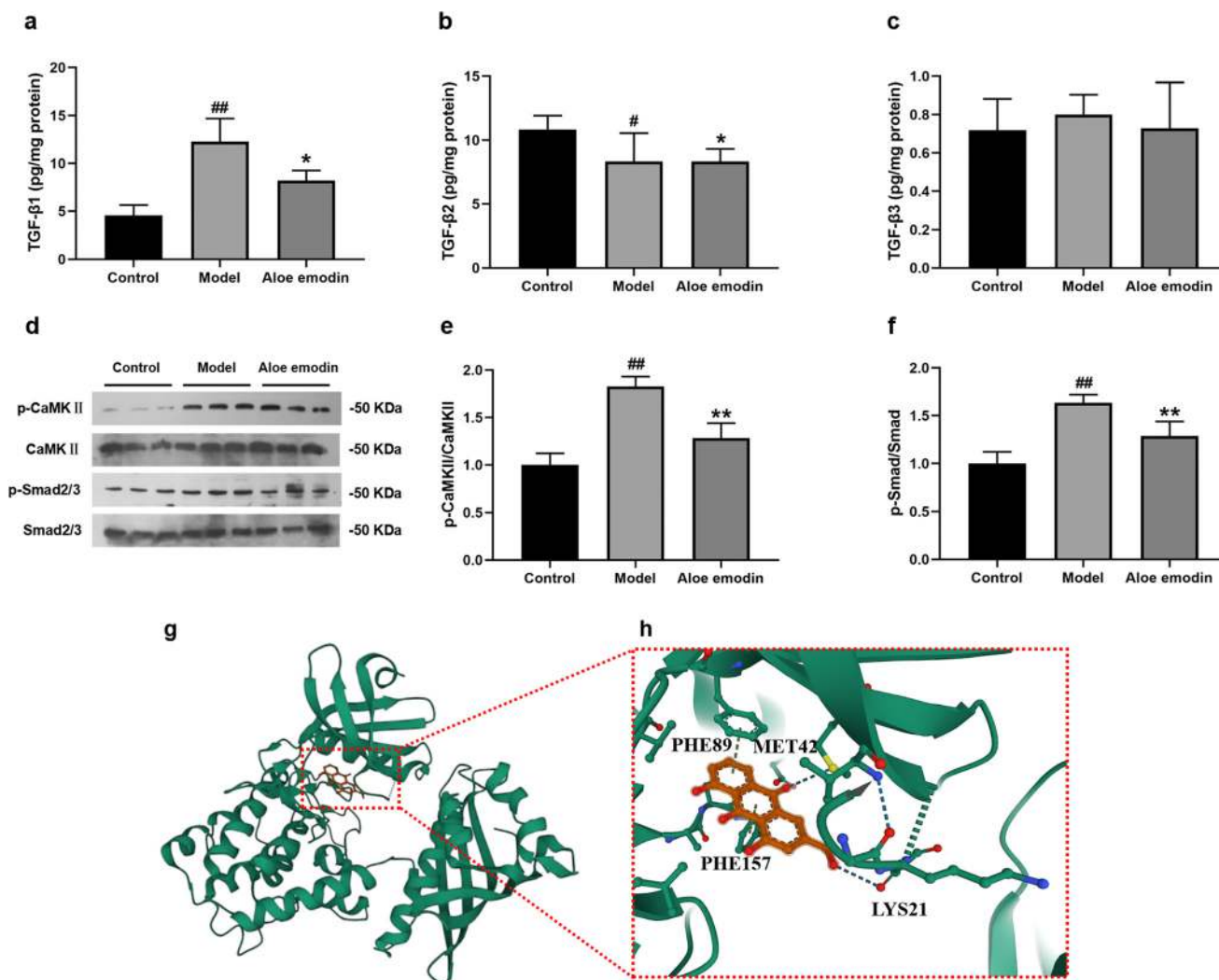


**Fig. 6** Effect of aloe emodin on TGF- $\beta$ s and CaMKII signaling in R6/1 mice. Aloe emodin treatment for 10 weeks significantly decreased the TGF- $\beta$ 1 content (a), the expression of p-CaMKII and the p-Smad2/3 level (d) in the cerebral cortex. Quantification of the band densities of p-CaMKII and p-Smad2/3 after aloe emodin treatment (e and f). Aloe emodin treatment had no effect on the contents of TGF- $\beta$ 2 (b). No significant differences in the contents of TGF- $\beta$ 3 were found among all groups (c). (g) Docking mode of aloe emodin with the protein crystal structure of CaMKII, key interactions of aloe emodin in the active site of CaMKII (PDB: 3SOA). (h) The binding pose of aloe emodin in the active site of CaMKII, where aloe emodin is highlighted in orange. All results are expressed as the mean  $\pm$  SD. TGF- $\beta$ ,  $n = 5-6$ ; WB,  $n = 5$ .  $^*p < 0.05$ ,  $^{##}p < 0.01$  vs. control;  $^*p < 0.05$ ,  $^{**}p < 0.01$  vs. model.

The up-regulation of dopamine receptors activated PKA, and increased the Thr 34 level of DARPP-32. Therefore, maybe aloe emodin can protect dopaminergic neurons against excitotoxicity.

TGF- $\beta$ 1, a multifunctional cytokine, participates in cell survival and microglial activation and is upstream of the Smad signal transduction pathway.<sup>32,33</sup> Current studies show that TGF- $\beta$ 1 regulates pathogenesis in several neurodegenerative disorders. AD, PD and amyotrophic lateral sclerosis patients display higher TGF- $\beta$ 1 content in serum and CSF than control patients.<sup>3</sup> However, the level of TGF- $\beta$ 1 in HD patients or animal models yielded contradictory results. With the aggravation of HD, TGF- $\beta$ 1-positive cells were increased in the brains of postmortem HD patients and colocalized with astrocytes.<sup>34</sup> The TGF- $\beta$  pathway was activated in human HD-induced pluri-

potent stem cells (hiPSCs).<sup>35</sup> Increasing TGF- $\beta$ 1 and p-SMAD2 levels were identified in iPSC-derived neural progenitor cells (NPCs) transfected with expanded CAG repeats.<sup>36</sup> In the hippocampus of a transgenic HD rat and R6/2 transgenic mice, the TGF- $\beta$  pathway was significantly activated.<sup>3</sup> In contrast, Battaglia *et al.* observed decreased TGF- $\beta$ 1 levels in HD patients.<sup>34</sup> In the cortex of YAC128 mice and R6/2 mice, TGF- $\beta$ 1 levels were reduced.<sup>34</sup> Therefore, we believe that additional studies should be performed to clarify the role of TGF- $\beta$ 1 in HD. CaMKII participates in synaptic plasticity and memory formation. On the one hand, CaMKII (T286) autophosphorylation maintains spatial memory formation and LTP; on the other hand, CaMKII promotes tau phosphorylation.<sup>37-39</sup> The excitatory neurons in CA1 exhibit high levels of CaMKII.<sup>40</sup> The lit-

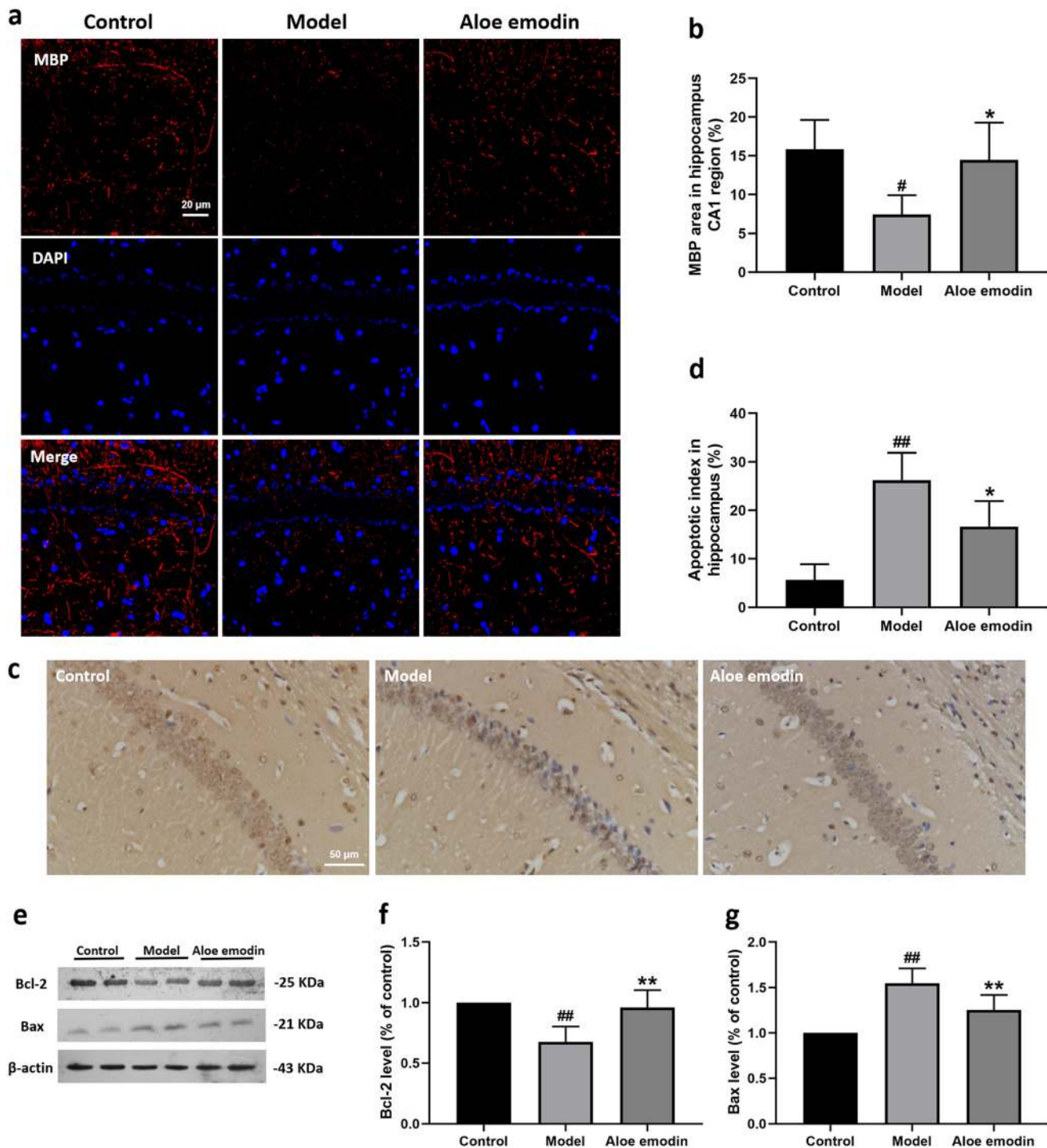


**Fig. 7** Effect of aloe emodin on apoptosis in the hippocampal area of R6/1 mice. Compared to the model group, aloe emodin increased the expression of MBP (a and b), decreased the number of TUNEL positive cells (c and d) in the hippocampal CA1 region, and also decreased the Bax/Bcl-2 expression ratio in the hippocampus (e–g). These results indicate that maybe aloe emodin prevented neuronal apoptosis in the hippocampus of R6/1 mice. All results are expressed as the mean  $\pm$  SD. Immunofluorescence and TUNEL,  $n = 4$ ; WB,  $n = 5$ .  $\#p < 0.05$ ,  $\#\#p < 0.01$  vs. control;  $*p < 0.05$ ,  $**p < 0.01$  vs. model.

erature has reported that inhibition of CaMKII also decreases p-Smad2/3 levels in human primary and pluripotent stem cells.<sup>41</sup>

Maybe inhibiting CaMKII/Smad and TGF- $\beta$ 1/Smad signaling is another potentially important function of aloe emodin.

Naturally, anthraquinone derivatives generally have the effect of inhibiting TGF- $\beta$ 1. Emodin shows an anti-fibrosis effect in renal fibrotic rats *via* inhibiting the TGF- $\beta$ 1/Smad7 pathway,<sup>42</sup> inhibits epithelial–mesenchymal transition induced by bleomycin in the lungs *via* suppressing the TGF- $\beta$ 1/Smad2/3.<sup>43</sup>

Emodin also inhibits the phosphorylation level and activity of CaMKII in renal ischemia-reperfusion injury models.<sup>44</sup> In this study, aloe emodin significantly decreased TGF- $\beta$ 1 levels and phosphorylation levels of Smad2/3 in R6/1 transgenic mice. However, no difference was found among any of the groups in the content of TGF- $\beta$ 2 or TGF- $\beta$ 3 of R6/1 mice. Active astrocytes and microglia showed strong TGF- $\beta$ 1 immunoreactivity. Therefore, we believe that inhibition of TGF- $\beta$ 1 downregulates the level of neuroinflammation, which may contribute to the anti-HD effect of aloe emodin. In this study, aloe emodin significantly decreased phosphorylation levels of CaMKII in R6/1 transgenic mice. Disruption of calcium homeostasis occurs not only in the brain but also in the peripheral tissues of HD patients.<sup>45</sup> Maybe, therefore, it is not just the brain that benefits from the regulation of calcium by aloe emodin. But we still do not know how dose aloe emodin block TGF- $\beta$  secretion. The mechanism of regulating TGF- $\beta$ 1 secretion is complex. For example, argonaute 2 activates TGF- $\beta$ 1 transcription and induces TGF- $\beta$ 1 production.<sup>46</sup> Inhibition of galectin-3 blocks TGF- $\beta$  secretion and attenuates the late-stage progression of lung fibrosis after bleomycin.<sup>47</sup> Inhibiting PKC activity prevents TGF- $\beta$ 1 transport.<sup>48</sup> The NF- $\kappa$ B signalling pathway can enhance the transcription of TGF- $\beta$ 1 in hepatic I/R injury.<sup>49</sup> There are also many microRNAs that can regulate the secretion and activity of TGF- $\beta$ .<sup>46,50–52</sup> Therefore, it may be difficult to find out what upstream target of aloe emodin inhibits TGF- $\beta$ 1 secretion. Maybe the RNA-seq method should be used in our next study.

## 5. Conclusions

Taken together, aloe emodin attenuated the motor and cognitive dysfunction in R6/1 mice. Aloe emodin also decreased the level of mutant huntingtin protein and inhibited CaMKII/Smad and TGF- $\beta$ 1/Smad signaling. The present study suggests that aloe emodin may be a promising candidate for use in HD and other neurodegenerative diseases.

## Ethical statement

All animal procedures were performed in accordance with the Guidelines for Care and Use of Laboratory Animals of “Shenyang Medical College” and approved by the Animal Ethics Committee of “Shenyang Medical College”.

## Author contributions

Conceptualization: Shuai Wang and Ge Jin. Data curation: Shuai Wang and Ying Yu. Formal analysis: Pengsheng Wei and Xue Li. Funding acquisition: Ge Jin. Investigation: Shuai Wang and Haotian Gao. Methodology: Shuai Wang, Haotian Gao and Jiaqi Chen. Project administration: Wang Yan. Resources: Nan Yan. Software: Jiahui Cao. Supervision: Shuyuan Liu and Ge Jin. Visualization: Shuai Wang. Writing—original draft: Nan

Yan and Shuai Wang. Writing—review and editing: Shuyuan Liu and Ge Jin. All authors have read and agreed to the published version of the manuscript.

## Conflicts of interest

There are no conflicts to declare.

## Acknowledgements

This work was supported by the Project of Liaoning Provincial Department of Education (SYXX202009), and the Project of Liaoning Provincial Department of Science and Technology (2021-MS-351).

## References

1. Á. Oliveira-Giacomelli, Y. Naaldijk, L. Sardá-Arroyo, M. C. B. Gonçalves, J. Corrêa-Velloso, M. M. Pillat, H. D. N. de Souza and H. Ulrich, Purinergic Receptors in Neurological Diseases With Motor Symptoms: Targets for Therapy, *Front. Pharmacol.*, 2018, **9**, 325, DOI: [10.3389/fphar.2018.00325](https://doi.org/10.3389/fphar.2018.00325).
2. T. Velusamy, A. S. Panneerselvam, M. Purushottam, M. Anusuyadevi, P. K. Pal, S. Jain, M. M. Essa, G. J. Guillemin and M. Kandasamy, Protective Effect of Antioxidants on Neuronal Dysfunction and Plasticity in Huntington's Disease, *Oxid. Med. Cell. Longevity*, 2017, 3279061, DOI: [10.1155/2017/3279061](https://doi.org/10.1155/2017/3279061).
3. K. H. Chang, Y. R. Wu, Y. C. Chen and C. M. Chen, Plasma inflammatory biomarkers for Huntington's disease patients and mouse model, *Brain, Behav., Immun.*, 2015, **44**, 121–127.
4. C. M. Guardia and S. W. Levison, Delayed ALK5 inhibition improves functional recovery in neonatal brain injury, *J. Cereb. Blood Flow Metab.*, 2017, **37**, 787–800.
5. R. Haque and A. Nazir, SMAD transcription factor, sma-9, attunes TGF-beta signaling cascade towards modulating amyloid beta aggregation and associated outcome in transgenic *C. Elegans*, *Mol. Neurobiol.*, 2016, **53**, 109–119.
6. S. Li, L. Yu, A. He and Q. Liu, Klotho Inhibits Unilateral Ureteral Obstruction-Induced Endothelial-to-Mesenchymal Transition via TGF- $\beta$ 1/Smad2/Snail1 Signaling in Mice, *Front. Pharmacol.*, 2019, **10**, 348, DOI: [10.3389/fphar.2019.00348](https://doi.org/10.3389/fphar.2019.00348).
7. C. Holmes, Review: systemic inflammation and Alzheimer's disease, *Neuropathol. Appl. Neurobiol.*, 2013, **39**, 51–68.
8. T. Wyss-Coray, C. Lin, D. A. Sanan, L. Mucke and E. Masliah, Chronic overproduction of transforming growth factor-beta1 by astrocytes promotes Alzheimer's disease-like microvascular degeneration in transgenic mice, *Am. J. Pathol.*, 2000, **156**, 139–150.
9. T. Wyss-Coray, C. Lin, D. von Eeuw, E. Masliah, L. Mucke and P. Lacombe, Alzheimer's disease-like cerebrovascular

- pathology in transforming growth factor-beta 1 transgenic mice and functional metabolic correlates, *Ann. N. Y. Acad. Sci.*, 2000, **903**, 317–323.
- 10 A. W. Deckel, R. Elder and G. Fuhrer, Biphasic developmental changes in Ca<sup>2+</sup>/calmodulin-dependent proteins in R6/2 Huntington's disease mice, *NeuroReport*, 2002, **13**, 707–711.
- 11 R. Russo, F. Cattaneo, P. Lippiello, C. Cristiano, F. Zurlo, M. Castaldo, C. Irace, T. Borsello, R. Santamaria, R. Ammendola, A. Calignano and M. C. Miniaci, Motor coordination and synaptic plasticity deficits are associated with increased cerebellar activity of NADPH oxidase, CAMKII, and PKC at preplaque stage in the TgCRND8 mouse model of Alzheimer's disease, *Neurobiol. Aging*, 2018, **68**, 123–133.
- 12 F. Dou, Y. Liu, L. Liu, J. Wang, T. Sun, F. Mu, Q. Guo, C. Guo, N. Jia, W. Liu, Y. Ding and A. Wen, Aloe-Emodin Ameliorates Renal Fibrosis Via Inhibiting PI3K/Akt/mTOR Signaling Pathway In Vivo and In Vitro, *Rejuvenation Res.*, 2019, **22**, 218–229.
- 13 X. Tang, Y. Zhang, X. Liu, X. Li, H. Zhao, H. Cui, Y. Shi, Y. Chen, H. Xu, Z. Meng, L. Zhao, H. Chen, Z. Wang, M. Zhu, Y. Lin, B. Yang and Y. Zhang, Aloe-emodin derivative produces anti-atherosclerosis effect by reinforcing AMBRA1-mediated endothelial autophagy, *Eur. J. Pharmacol.*, 2022, **916**, 174641, DOI: [10.1016/j.ejphar.2021.174641](https://doi.org/10.1016/j.ejphar.2021.174641).
- 14 G. Cheng, Z. Pi, X. Zhuang, Z. Zheng, S. Liu, Z. Liu and F. Song, The effects and mechanisms of aloe-emodin on reversing adriamycin-induced resistance of MCF-7/ADR cells, *Phytother. Res.*, 2021, **35**, 3886–3897.
- 15 M. Xian, J. Cai, K. Zheng, Q. Liu, Y. Liu, H. Lin, S. Liang and S. Wang, Aloe-emodin prevents nerve injury and neuroinflammation caused by ischemic stroke via the PI3K/AKT/mTOR and NF-kappaB pathway, *Food Funct.*, 2021, **12**, 8056–8067.
- 16 R. R. Li, X. F. Liu, S. X. Feng, S. N. Shu, P. Y. Wang, N. Zhang, J. S. Li and L. B. Qu, Pharmacodynamics of Five Anthraquinones (Aloe-emodin, Emodin, Rhein, Chrysophanol, and Physcion) and Reciprocal Pharmacokinetic Interaction in Rats with Cerebral Ischemia, *Molecules*, 2019, **24**, 1898, DOI: [10.3390/molecules24101898](https://doi.org/10.3390/molecules24101898).
- 17 S. Ahmad, A. Khan, W. Ali, M. H. Jo, J. Park, M. Ikram and M. O. Kim, Fisetin Rescues the Mice Brains Against D-Galactose-Induced Oxidative Stress, Neuroinflammation and Memory Impairment, *Front. Pharmacol.*, 2021, **12**, 612078, DOI: [10.3389/fphar.2021.612078](https://doi.org/10.3389/fphar.2021.612078).
- 18 S. Khatoun, N. B. Agarwal, M. Samim and O. Alam, Neuroprotective Effect of Fisetin Through Suppression of IL-1R/TLR Axis and Apoptosis in Pentylentetrazole-Induced Kindling in Mice, *Front. Neurol.*, 2021, **12**, 689069, DOI: [10.3389/fneur.2021.689069](https://doi.org/10.3389/fneur.2021.689069).
- 19 P. Maher, T. Akaishi and K. Abe, Flavonoid fisetin promotes ERK-dependent long-term potentiation and enhances memory, *Proc. Natl. Acad. Sci. U. S. A.*, 2006, **103**(44), 16568–16573.
- 20 S. J. Guyenet, S. A. Furrer, V. M. Damian, T. D. Baughan, A. R. La Spada and G. A. Garden, A simple composite phenotype scoring system for evaluating mouse models of cerebellar ataxia, *J. Visualized Exp.*, 2010, 1787, DOI: [10.3791/1787](https://doi.org/10.3791/1787).
- 21 P. Liu, Y. Li, W. Yang, D. Liu, X. Ji, T. Chi, Z. Guo, L. Li and L. Zou, Prevention of Huntington's Disease-Like Behavioral Deficits in R6/1 Mouse by Tolfenamic Acid Is Associated with Decreases in Mutant Huntingtin and Oxidative Stress, *Oxid. Med. Cell. Longevity*, 2019, 4032428, DOI: [10.1155/2019/4032428](https://doi.org/10.1155/2019/4032428).
- 22 P. Maher, R. Dargusch, L. Bodai, P. E. Gerard, J. M. Purcell and J. L. Marsh, ERK activation by the polyphenols fisetin and resveratrol provides neuroprotection in multiple models of Huntington's disease, *Hum. Mol. Genet.*, 2011, **20**(2), 261–270.
- 23 V. Brito, A. Giral, M. Masana, A. Royes, M. Espina, E. Sieiro, J. Alberch, A. Castañé, J. A. Girault and S. Ginés, Cyclin-Dependent Kinase 5 Dysfunction Contributes to Depressive-like Behaviors in Huntington's Disease by Altering the DARPP-32 Phosphorylation Status in the Nucleus Accumbens, *Biol. Psychiatry*, 2019, **86**, 196–207.
- 24 M. Fjodorova, M. Louessard, Z. Li, D. C. De La Fuente, E. Dyke, S. P. Brooks, A. L. Perrier and M. Li, CTIP2-Regulated Reduction in PKA-Dependent DARPP32 Phosphorylation in Human Medium Spiny Neurons: Implications for Huntington Disease, *Stem Cell Rep.*, 2019, **13**, 448–457.
- 25 J. Zhang, X. Sun, S. Zheng, X. Liu, J. Jin, Y. Ren and J. Luo, Myelin basic protein induces neuron-specific toxicity by directly damaging the neuronal plasma membrane, *PLoS One*, 2014, **9**, e108646, DOI: [10.1371/journal.pone.0108646](https://doi.org/10.1371/journal.pone.0108646).
- 26 Z. Yan, L. Chu, X. Jia, L. Lin and S. Cheng, Myelin basic protein enhances axonal regeneration from neural progenitor cells, *Cell Biosci.*, 2011, **11**, 80, DOI: [10.1186/s13578-021-00584-7](https://doi.org/10.1186/s13578-021-00584-7).
- 27 X. Dong, J. Fu, X. Yin, S. Cao, X. Li, L. Lin, M. N. Huyilgeqi and J. Ni, Emodin: A Review of its Pharmacology, Toxicity and Pharmacokinetics, *Phytother. Res.*, 2016, **30**, 1207–1218.
- 28 M. Anglada-Huguet, X. Xifró, A. Giral, A. Zamora-Moratalla, E. D. Martín and J. Alberch, Prostaglandin E2 EP1 receptor antagonist improves motor deficits and rescues memory decline in R6/1 mouse model of Huntington's disease, *Mol. Neurobiol.*, 2014, **49**, 784–795.
- 29 F. Kreilaus, A. S. Spiro, A. J. Hannan, B. Garner and A. M. Jenner, Therapeutic Effects of Anthocyanins and Environmental Enrichment in R6/1 Huntington's Disease Mice, *J. Huntington's Dis.*, 2016, **5**, 285–296.
- 30 H. Kalonia, P. Kumar, A. Kumar and B. Nehru, Protective effect of montelukast against quinolinic acid/malonic acid induced neurotoxicity: possible behavioral, biochemical, mitochondrial and tumor necrosis factor- $\alpha$  level alterations in rats, *Neuroscience*, 2010, **171**, 284–299.

- 31 J. Y. Shin, Z. H. Fang, Z. X. Yu, C. E. Wang, S. H. Li and X. J. Li, Expression of mutant huntingtin in glial cells contributes to neuronal excitotoxicity, *J. Cell Biol.*, 2005, **171**, 1001–1012.
- 32 K. R. Bowles, T. Stone, P. Holmans, N. D. Allen, S. B. Dunnett and L. Jones, SMAD transcription factors are altered in cell models of HD and regulate HTT expression, *Cell. Signalling*, 2016, **31**, 1–14.
- 33 T. C. Brionne, I. Tesseur, E. Masliah and T. Wyss-Coray, Loss of TGF-beta 1 leads to increased neuronal cell death and microgliosis in mouse brain, *Neuron*, 2003, **40**, 1133–1145.
- 34 G. Battaglia, M. Cannella, B. Riozzi, S. Orobello, M. L. Maat-Schieman, E. Aronica, C. L. Busceti, A. Ciarmiello, S. Alberti, E. Amico, J. Sassone, S. Sipione, V. Bruno, L. Frati, F. Nicoletti and F. Squitieri, Early defect of transforming growth factor beta1 formation in Huntington's disease, *J. Cell. Mol. Med.*, 2011, **15**, 555–571.
- 35 M. C. An, N. Zhang, G. Scott, D. Montoro, T. Wittkop, S. Mooney, S. Melov and L. M. Ellerby, Genetic correction of Huntington's disease phenotypes in induced pluripotent stem cells, *Cell Stem Cell*, 2012, **2012**, 253–263.
- 36 K. L. Ring, M. C. An, N. Zhang, R. N. O'Brien, E. M. Ramos, F. Gao, R. Atwood, B. J. Bailus, S. Melov, S. D. Mooney, G. Coppola and L. M. Ellerby, Genomic analysis reveals disruption of striatal neuronal development and therapeutic targets in human Huntington's disease neural stem cells, *Stem Cell Rep.*, 2015, **5**, 1023–1038.
- 37 K. P. Giese, N. B. Fedorov, R. K. Filipkowski and A. J. Silva, Autophosphorylation at Thr286 of the alpha calcium-calmodulin kinase II in LTP and learning, *Science*, 1998, **279**, 870–873.
- 38 A. C. Need and K. P. Giese, Handling and environmental enrichment do not rescue learning and memory impairments in alphaCamKII(T286A) mutant mice, *Genes, Brain Behav.*, 2003, **2**, 132–139.
- 39 Y. Wei, C. Han, Y. Wang, B. Wu, T. Su, Y. Liu and R. He, Ribosylation triggering Alzheimer's disease-like Tau hyperphosphorylation via activation of CaMKII, *Aging Cell*, 2015, **14**, 754–763.
- 40 A. Ghosh and K. P. Giese, Calcium/calmodulin-dependent kinase II and Alzheimer's disease, *Mol. Brain*, 2015, **8**, 78, DOI: [10.1186/s13041-015-0166-2](https://doi.org/10.1186/s13041-015-0166-2).
- 41 B. Saitta, J. Elphingstone, S. Limfat, R. Shkhyan and D. Evseenko, CaMKII inhibition in human primary and pluripotent stem cell-derived chondrocytes modulates effects of TGFβ and BMP through SMAD signaling, *Osteoarthritis Cartilage*, 2019, **27**, 158–171.
- 42 L. Ma, H. Li, S. Zhang, X. Xiong, K. Chen, P. Jiang, K. Jiang and G. Deng, Emodin ameliorates renal fibrosis in rats via TGF-beta1/Smad signaling pathway and function study of Smurf 2, *Int. Urol. Nephrol.*, 2018, **50**, 373–382.
- 43 S. L. Tian, Y. Yang, X. L. Liu and Q. B. Xu, Emodin Attenuates Bleomycin-Induced Pulmonary Fibrosis via Anti-Inflammatory and Anti-Oxidative Activities in Rats, *Med. Sci. Monit.*, 2018, **24**, 1–10.
- 44 Y. Wang, Q. Liu, J. Cai, P. Wu, D. Wang, Y. Shi, T. Huyan, J. Su, X. Li, Q. Wang, H. Wang, F. Zhang, O. N. Bae and L. Tie, Emodin prevents renal ischemia-reperfusion injury via suppression of CAMKII/DRP1-mediated mitochondrial fission, *Eur. J. Pharmacol.*, 2022, **916**, 174603, DOI: [10.1016/j.ejphar.2021.174603](https://doi.org/10.1016/j.ejphar.2021.174603).
- 45 J. V. Joviano-Santos, A. Santos-Miranda, A. Botelho, I. de Jesus, J. N. Andrade, T. de Oliveira Barreto, M. Magalhães-Gomes, P. Valadão, J. Cruz, M. M. Melo, S. Guatimosim and C. Guatimosim, Increased oxidative stress and CaMKII activity contribute to electro-mechanical defects in cardiomyocytes from a murine model of Huntington's disease, *FEBS J.*, 2019, **286**, 110–123.
- 46 L. Wang, X. Du, Q. Li, W. Wu, Z. Pan and Q. Li, miR-2337 induces TGF-β1 production in granulosa cells by acting as an endogenous small activating RNA, *Cell Death Discovery*, 2021, **7**(1), 253, DOI: [10.1038/s41420-021-00644-4](https://doi.org/10.1038/s41420-021-00644-4).
- 47 A. C. Mackinnon, M. A. Gibbons, S. L. Farnworth, H. Leffler, U. J. Nilsson, T. Delaine, A. J. Simpson, S. J. Forbes, N. Hirani, J. Gaudie and T. Sethi, Regulation of transforming growth factor-β1-driven lung fibrosis by galectin-3, *Am. J. Respir. Crit. Care Med.*, 2012, **185**(5), 537–546.
- 48 F. Zhang, W. Dong, W. Zeng, L. Zhang, C. Zhang, Y. Qiu, L. Wang, X. Yin, C. Zhang and W. Liang, Naringenin prevents TGF-β1 secretion from breast cancer and suppresses pulmonary metastasis by inhibiting PKC activation, *Breast Cancer Res.*, 2016, **18**(1), 38, DOI: [10.1186/s13058-016-0698-0](https://doi.org/10.1186/s13058-016-0698-0).
- 49 J. Cao, T. Xu, C. Zhou, S. Wang, B. Jiang, K. Wu and L. Ma, NR4A1 knockdown confers hepatoprotection against ischaemia-reperfusion injury by suppressing TGFβ1 via inhibition of CYR61/NF-κB in mouse hepatocytes, *J. Cell. Mol. Med.*, 2021, **25**(11), 5099–5112.
- 50 Y. Du, Y. T. Yang, G. Tang, J. S. Jia, N. Zhu and W. J. Yuan, Butyrate alleviates diabetic kidney disease by mediating the miR-7a-5p/P311/TGF-β1 pathway, *FASEB J.*, 2020, **34**(8), 10462–10475.
- 51 S. Zhang and S. Pan, miR-124-3p targeting of TGF-β1 inhibits the proliferation of hypertrophic scar fibroblasts, *Adv. Clin. Exp. Med.*, 2021, **30**(3), 263–271.
- 52 X. Du, L. Wang, Q. Li, W. Wu, P. Shang, Y. Chamba, Z. Pan and Q. Li, miR-130a/TGF-β1 axis is involved in sow fertility by controlling granulosa cell apoptosis, *Theriogenology*, 2020, **157**, 407–417.